MOLECULAR ECOLOGY

Molecular Ecology (2016) **25**, 3912–3928 doi: 10.1111/mec.13724

Divergence history of the Carpathian and smooth newts modelled in space and time

P. ZIELIŃSKI,* K. NADACHOWSKA-BRZYSKA,† K. DUDEK* and W. BABIK*

Institute of Environmental Sciences, Jagiellonian University, Gronostajowa 7, 30-387 Kraków, Poland, †Department of Evolutionary Biology, Uppsala University, Norbyvägen 18D, 75236 Uppsala, Sweden

Abstract

Information about demographic history is essential for the understanding of the processes of divergence and speciation. Patterns of genetic variation within and between closely related species provide insights into the history of their interactions. Here, we investigated historical demography and genetic exchange between the Carpathian (*Lissotriton montandoni*, Lm) and smooth (*L. vulgaris*, Lv) newts. We combine an extensive geographical sampling and multilocus nuclear sequence data with the approximate Bayesian computation framework to test alternative scenarios of divergence and reconstruct the temporal and spatial pattern of gene flow between species. A model of recent (last glacial period) interspecific gene flow was favoured over alternative models. Thus, despite the relatively old divergence (4–6 mya) and presumably long periods of isolation, the species have retained the ability to exchange genes. Nevertheless, the low migration rates (ca. 10^{-6} per gene copy per generation) are consistent with strong reproductive isolation between the species. Models allowing demographic changes were favoured, suggesting that the effective population sizes of both species at least doubled as divergence reaching the current ca. 0.2 million in Lm and 1 million in Lv. We found asymmetry in rates of interspecific gene flow between Lm and one evolutionary lineage of Lv. We suggest that intraspecific polymorphism for hybrid incompatibilities segregating within Lv could explain this pattern and propose further tests to distinguish between alternative explanations. Our study highlights the importance of incorporating intraspecific genetic structure into the models investigating the history of divergence.

Keywords: ABC, asymmetric introgression, demographic history, gene flow, *Lissotriton*, newt

Received 14 October 2015; revision received 1 June 2016; accepted 1 June 2016

Introduction

The process of speciation, defined as the development of reproductive isolation between populations, may occur in complete geographical isolation or in the face of unrestricted gene flow (Coyne & Orr 2004; Seehausen *et al.* 2014). These two extremes are linked via a continuum of intermediate situations where gene exchange may be restricted temporally, spatially and may occur in some parts of the genome but not in the others (Mallet 2007; Nosil 2008; Pinho & Hey 2010; Feder *et al.* 2012; Abbott *et al.* 2013). Even if speciation is initiated in isolation, the time required for the evolution of complete reproductive isolation can be very long, reaching millions of generations (Hewitt 2011; Abbott *et al.* 2013). Often, environmental changes causing shifts of species ranges are more rapid, as was the case during the Pleistocene climatic oscillations (Hewitt 2004, 2011). Such range changes may lead to contact and interbreeding between incompletely reproductively isolated species (Hewitt 2011; Hoffmann & Sgro 2011; Abbott *et al.* 2013). As long as differentiating populations are able to produce viable and fertile hybrid offspring which backcrosses to the parental species, interspecific gene flow will ensue (Mallet 2005). Studies of the genetic exchange

Correspondence: Piotr Zieliński, Fax: +48 12 664 69 12; E-mail: piotr.zielinski@uj.edu.pl

between incompletely isolated species provided important contributions to the understanding of speciation (Yatabe *et al.* 2007; Nosil *et al.* 2008; Teeter *et al.* 2010; Kronforst *et al.* 2013; Nadachowska-Brzyska *et al.* 2013; Roux *et al.* 2013; Poelstra *et al.* 2014). However, some outstanding questions regarding the build-up of genomic differentiation between diverging species and the impact of gene flow on the process of speciation remain unanswered (Abbott *et al.* 2013; Seehausen *et al.* 2014).

Major questions that still need to be addressed include the temporal pattern of gene flow between differentiating species and the relationship between patterns of gene flow and intraspecific genetic structure. First, the recognition of the temporal pattern of gene flow between differentiating species holds the potential to resolve the long-standing issue of the role of gene exchange in species formation and in shaping patterns of variation and diversity (Pinho & Hey 2010). Second, the genetic architecture of isolation between a pair of taxa may vary spatially due to environmental, ecological or genetic variation in factors that contribute to isolation, resulting in geographically variable interspecific gene flow (Nolte *et al.* 2009; Teeter *et al.* 2010). For instance, genetic differences accumulated during the divergence may result in negative epistatic interactions, known as Bateson–Dobzhansky–Muller incompatibilities, causing low fitness of hybrids (Bateson 1909; Dobzhansky 1936; Muller & Pontecorvo 1942). If some populations within species harbour fewer alleles incompatible with alleles of another species, then introgression following hybridization involving these populations may be easier because intrinsic selection against hybrids would be weaker (Cutter 2012; Corbett-Detig *et al.* 2013). Thus, variable patterns of introgression may indicate intraspecific variation at loci responsible for interspecific reproductive isolation (Cutter 2012).

The quantitative characterization of the patterns of gene flow between differentiating species is required to understand the process of divergence (Pinho & Hey 2010; Sousa & Hey 2013). However, histories of various parts of the genome may differ, simply due to stochasticity of the coalescent process or because strength of gene flow may vary depending on linkage to regions underlying reduced fitness of hybrids (Barton & Bengtsson 1986). Thus, only data collected from multiple genomic regions can provide reliable and quantitative information about the historical and contemporary gene flow between differentiating taxa (Edwards & Beerli 2000; Sousa & Hey 2013). A wide range of approaches have been developed to reconstruct demographic history of species (Sousa & Hey 2013). Approximate Bayesian computation (ABC; Beaumont *et al.* 2002) is an approach, which has recently gained in popularity. ABC methods are flexible and allow inferences under complex demographic models, because the exact likelihood calculation is bypassed by using summary statistics to characterize patterns of variation in the data (Bertorelle *et al.* 2010; Csillery *et al.* 2010). ABC methods are useful for differentiating between various models of species divergence, for instance, between speciation models allowing or ruling out the postdivergence gene flow (Sousa *et al.* 2012; Sousa & Hey 2013).

In this study, we use the ABC approach to investigate the history of two sister salamandrid species: the Carpathian (*Lissotriton montandoni*, Lm) and the smooth newt (*L. vulgaris*, Lv). Molecular and fossil data suggest pre-Pleistocene divergence (Rafinski & Arntzen 1987; Roček 1994; Babik *et al.* 2005; Pabijan *et al.* 2015). The species are easy to distinguish in the field due to differences in coloration (e.g. unspotted belly in Lm vs. spotted in Lv), male secondary sexual characters (denticulate crest and toe flaps in Lv vs. tail filament, no crest or toe flaps in Lm) and body shape (Babik & Rafiński 2004). The Carpathian newt is endemic to the Carpathians and easternmost Sudetes Mountains. The smooth newt is widely distributed in Eurasia ranging from western Europe to western Siberia and comprises several morphologically and genetically differentiated groups (Rafiński *et al.* 2001; Babik *et al.* 2005; Nadachowska & Babik 2009; Pabijan *et al.* 2015). Substantial premating reproductive isolation was found in a hybrid zone and microsatellite data show little evidence of recent interspecific nuclear gene flow at a broader geographical scale (Babik *et al.* 2003; Zieliński *et al.* 2013). However, the complete replacement of Lm mitochondrial DNA by several mtDNA lineages derived from Lv suggests prolonged history of hybridization and gene flow between species (Babik *et al.* 2005; Zieliński *et al.* 2013). Evidence from a panel of SNP markers (Zieliński *et al.* 2014a) and MHC class II genes (Nadachowska-Brzyska *et al.* 2012) points to limited, genomically and spatially heterogeneous interspecific gene flow in the nuclear genome.

The pattern of contemporary hybridization revealed by previous studies is only a single snapshot of a complex history of interaction between the differentiating species. Therefore, in this study, we set out to provide a long-term perspective on the process of interspecific gene flow, its spatial and temporal variation. Several alternative scenarios of the Lm and Lv divergence history were tested using multilocus nuclear sequence data. Because of previously detected massive mtDNA introgression, we hypothesized substantial historical gene flow also in the nuclear genome and expected its asymmetry. To test whether patterns of gene flow correlate with intraspecific genetic structuring, we incorporated the latter into the analyses.

Materials and methods

Sampling and markers

We sampled 31 populations of Lm (39 individuals) and 38 populations of Lv (45 individuals) (Fig. 1 and Table S1, Supporting information). Newts were sampled in water during the breeding season; individual ponds were treated as local populations. Samples of Lm covered the entire species range, whereas populations of Lv were sampled in the areas surrounding the Lm range but extending far beyond the area of sympatry. Samples from syntopic populations (ponds where both species co-occur) were not analysed to exclude the effect of ongoing hybridization and early-generation hybrids. To characterize sequence variation and differentiation, we used data acquired from ca. 500-bp fragments of the last exon of 74 protein-coding genes (poly data set). These markers include mostly 3′ untranslated regions (3′UTR), are single copy and do not show evidence of null alleles (Zieliński *et al.* 2014b). Markers were amplified and analysed as described in Zieliński *et al.* (2014b). Linkage disequilibrium was tested in GENEPOP 4.1.2 (Rousset 2008); the type I error was controlled using the false discovery rate (FDR) approach implemented in QVALUE (Storey 2002; Storey & Tibshirani 2003). For the ABC analysis, we further excluded eight markers that were fully coding (*arh*, *cnppd*, *rbm*, *znf4*) or amplified inconsistently (*cep*, *fam178*, *myo7*, *scf1*), so that the final data set included 66 markers. Protein-coding parts of the markers and alignment columns containing gaps were removed. Individuals in which more than 10% markers did not amplify were removed from the analysis. Finally, the data set was subsampled to the lowest number of observations per locus; thus, our final ABC data set contained 58 populations, 26 Lm and 32 Lv (Fig. S1, Supporting information). Smooth newt populations were assigned to two evolutionary lineages (groups), inside (LvIN) and outside (LvOUT) the Carpathian basin. These two lineages are deeply diverged in mtDNA, nuclear microsatellites and SNPs and show some morphological differentiation (Babik *et al.* 2005; Zieliński *et al.* 2013, 2014a). While Lm is also genetically structured, this structure is relatively shallow (Zieliński *et al.* 2013, 2014a), and thus, here we consider all Lm as a single genetic lineage. To minimize the confounding effects of population structure, we randomly subsampled one gene copy per population, resulting in 26 Lm and 32 Lv gene copies per locus in the ABC data set. We assume that newt breeding ponds correspond to discrete demes, which may undergo extinction and recolonization, and thus, the set of regional populations can be considered a metapopulation. It has been shown (Wakeley & Aliacar 2001; Wakeley 2004) that if one gene copy per locus is sampled per deme in a metapopulation composed of a large number of demes, the ancestral process producing such a sample is identical to the unstructured coalescent process.

Polymorphism and population differentiation

The extent of DNA polymorphism within species and populations was measured by nucleotide diversity, that is the average fraction of nucleotide positions differing between a pair of homologous sequences within a group, denoted as π (Nei & Li 1979). Nucleotide

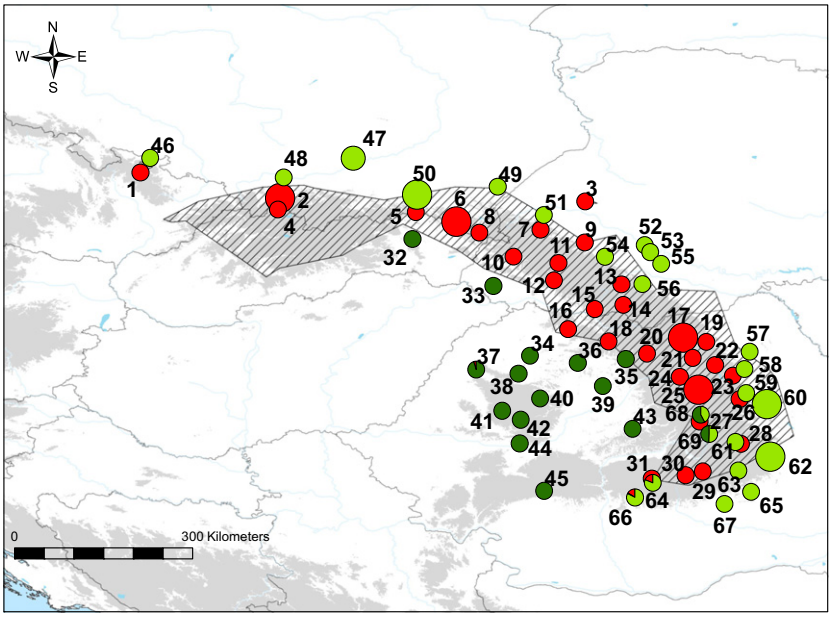

Fig. 1 The distribution of sampling localities (details in Table S1, Supporting information) and genetic structuring inferred by Structure from 74 sequence loci for $K = 3$. Symbol areas are proportional to sample sizes. Grey – Lm, light grey – LvOUT, dark grey – LvIN. The distribution of *L. montandoni* is hatched; populations 1 and 3 are isolated from the continuous part of the range. Areas above 500 m a.s.l. are shaded.

divergence between populations was measured using average fraction of pairwise differences (d_{XY}) and net nucleotide divergence (d_A; Nei & Kumar 2000; Nei & Li 1979). All polymorphism measures were calculated in MSTATSPOP v.0.998980beta (S. E. Ramos-Onsins, L. Ferretti, E. Raineri, G. Marmorini, W. Burgos & G. Vera, unpublished, available at http://bioinformatics.cragenomica.es/numgenomics/people/sebas/software/software.html). Differentiation between species and populations was measured by F_{ST}, which was calculated using Weir & Cockerham's (1984) approach based on the analysis of molecular variance, implemented in Arlequin with pairwise differences as the measure of genetic distance (Excoffier & Lischer 2010). As we sampled one to three individuals per population, we treated F_{ST} as an empirical measure of differentiation and did not test its significance in pairwise comparisons within species. F_{ST} and the measures of polymorphism and divergence mentioned above were calculated on the poly data set with the sequences of all markers concatenated. Intraspecific nucleotide diversity (π) and Tajima's D (D; Tajima 1989) were calculated for each gene separately, to assess the variation across markers; significance of Tajima's D in each species was tested with coalescent simulations under the standard neutral model. F_{ST} and the numbers of nucleotide differences between and within populations were visualized using R (R Development Core Team 2011).

To infer the number of genetic clusters present in the data set, we used the Bayesian clustering method implemented in STRUCTURE 2.3.3 (Pritchard *et al.* 2000; Falush *et al.* 2007; Hubisz *et al.* 2009); entire haplotypes were treated as alleles at each locus. We ran Structure under the admixture model with uncorrelated allele frequencies. We examined K values from 1 to 15 with 10 replicate runs for each K and 250 000 burn-in steps followed by a million post-burn-in MCMC iterations. To infer the most likely number of clusters, we used the averaged posterior probability of the data given K clusters (Pritchard *et al.* 2000) and ΔK, a measure of second-order rate of change in the likelihood of K (Evanno *et al.* 2005), using the online software STRUCTURE HARVESTER (Earl & vonHoldt 2012).

Summary statistics for ABC

Summary statistics are quantities calculated from the data to represent the maximum amount of the information present in the data in the simplest possible form (Csillery *et al.* 2010). If summary statistics adequately capture information about the model parameters contained in the data, then posterior distributions of the model parameters are highly informative. It might seem that increasing the number of summary statistics should increase the amount of available information. However, it was shown that the larger the number of summary statistics, the larger the statistical noise included in the posterior estimation (Joyce & Marjoram 2008). Indeed, Wegmann *et al.* (2009) showed that when too many summary statistics are included, the obtained posteriors may be biased. Thus, we decided to focus on a set of basic summary statistics likely to be informative about both gene flow between and demography within species: number of segregating sites (S), number of fixed polymorphisms (SF), number of shared polymorphisms (SS), number of polymorphisms private to each species/group of populations (SP), F_{ST} calculated between species/groups of populations and between a given group and the remaining groups pooled (in three-population models, see below), Tajima's D (D) and nucleotide diversity (π). The last two were calculated both within each group and for the whole data set. Summary statistics for both observed and simulated data sets were calculated on polymorphic biallelic sites only, positions with more than two segregating variants were excluded as departing from the infinite sites model. Calculations were performed using MSTATSPOP v.0.998980-beta. Following Wegmann *et al.* (2009), to reduce the dimensionality of the summary statistics space, we also calculated the partial least-squares (PLS) regression (Boulesteix & Strimmer 2007). PLS-transformed statistics were used to calculate the Euclidean distance between observed and simulated data sets and to retain simulations that were closest to the observed data. We investigated 5–7 PLS components in three-population models and 4–6 in two-population models. Simulations retained using PLS components and untransformed summary statistics gave very similar results in both model selection and parameter estimation. Thus, we present results obtained with untransformed statistics.

Demographic models

We tested various scenarios of species divergence regarding the extent, direction and timing of interspecific gene flow in the context of intraspecific structuring. Because historical demographic changes may affect inferences about gene flow, we analysed also models allowing such changes. Smooth newts inhabiting areas surrounding the Carpathian newt range are deeply structured genetically into two groups (Zieliński *et al.* 2014a). It was shown that not accounting for population structure might introduce false signals of population size changes (Chikhi *et al.* 2010), whereas migration from unsampled populations can introduce serious bias in population size estimates (Beerli 2004). Thus, we started with three-population models, which potentially provide the most comprehensive picture of the divergence history. However, due to a

large number of parameters that need to be estimated, three-population models may become highly complex and intractable (Aeschbacher *et al.* 2013). Thus, we intended to analyse only simple scenarios using three-population models. To reduce the dimensionality of the parameter space and increase the accuracy of estimation, we also analysed pairwise models. Such models allowed analysis of the alternative scenarios regarding the temporal aspects of gene flow under constant and variable population sizes.

We built seven models with three descendant populations (Fig. S2, Supporting information). No demographic changes or changes in historical gene flow were allowed to keep the models as simple as possible. The first model (M1), assumed no gene flow between any of the populations, whereas all other models allowed constant migration between some or all populations. The second model (M2) allowed migration between the Lv groups only. Two models (M3 and M4) allowed for migration between the Lv groups and between LvIN or LvOUT and Lm, respectively. Two models (M5 and M6) assumed only migration between Lm and LvIN or LvOUT, respectively. Finally, model seven (M7) allowed for migration between all three groups.

The two-population models were constructed for the following pairs: (i) Lm and Lv (LvIN and LvOUT combined), (ii) Lm and LvIN, (iii) Lm and LvOUT and (iv) LvIN and LvOUT. For each pairwise comparison, we tested 12 demographic models (Fig. 2): six scenarios of gene flow, each either under constant population size (CS)

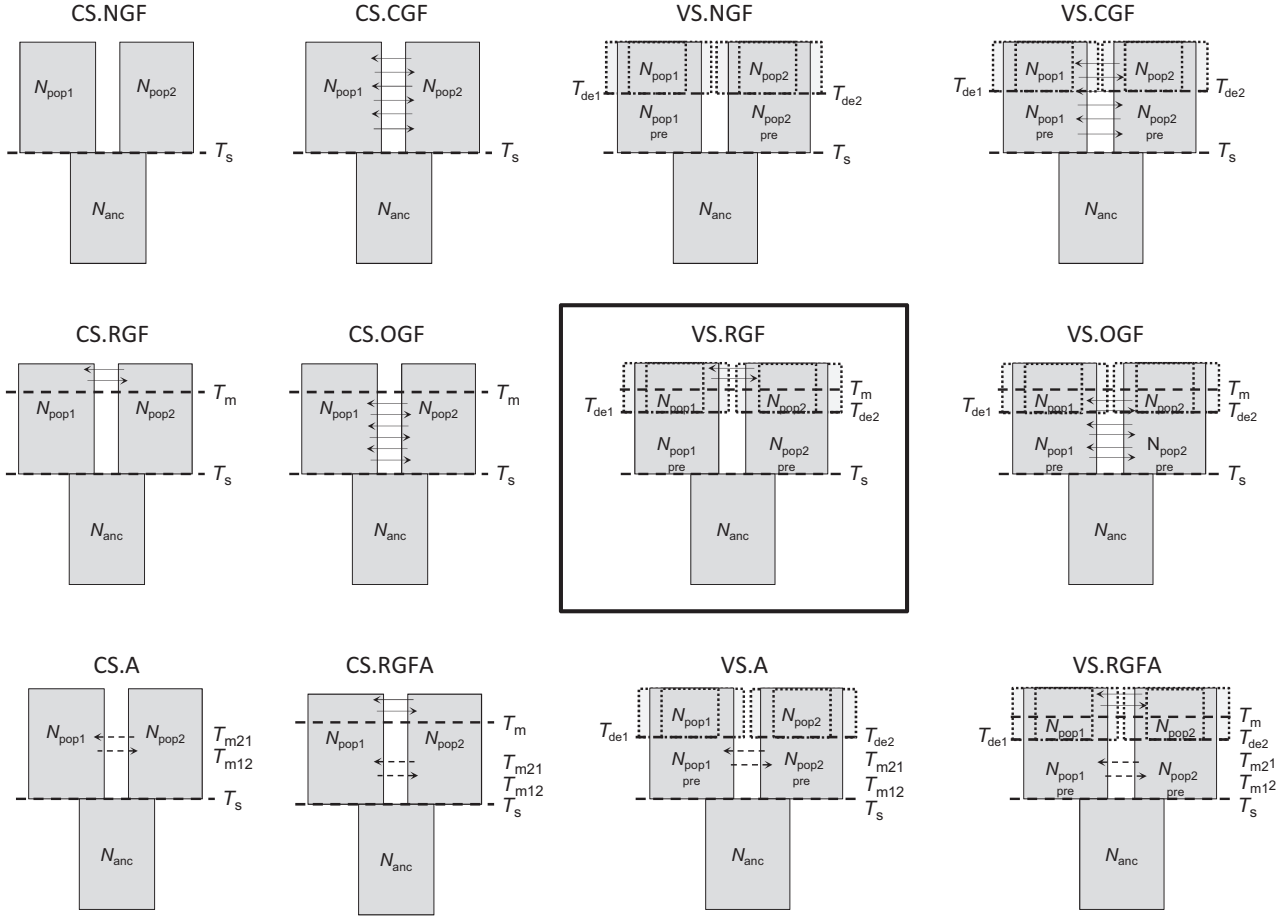

Fig. 2 The two-group models investigated. Models were constructed for the following groups: (i) Lm and Lv (combined LvIN and LvOUT), (ii) Lm and LvIN, (iii) Lm and LvOUT and (iv) LvIN and LvOUT. Six scenarios of gene flow were analysed (NGF – no gene flow, CGF – constant gene flow, RGF – recent (last 200 kya) gene flow, A – single instantaneous admixture event at any time after the divergence, RGFA – recent gene flow plus single admixture event older than 200 kya, OGF – old (older than 200 kya) gene flow), each under constant population size (CS) or a single demographic change (VS). The frame indicates the best model in all pairwise comparisons. N_{pop1}, N_{pop2}, $N_{pop1pre}$, $N_{pop2pre}$ and N_{anc} – population size of group 1, group 2, group 1 before demographic change, group 2 before demographic change and ancestral population, respectively. T_S – time of split. T_{de1} and T_{de2} – time of demographic change in group 1 and group 2, respectively. T_m – time of migration. T_{m21} and T_{m12} – time of instantaneous admixture of genes from group 2 to group 1 and conversely. Constant arrows indicate migration whereas dotted admixture.

or allowing a single demographic change (VS) in both descendant populations. The six scenarios were as follows: (i) no gene flow (NGF), (ii) constant gene flow (CGF), (iii) recent (last 200 kya) gene flow (RGF), (iv) single instantaneous admixture event at any time after the divergence (A), (v) recent gene flow plus single admixture event older than 200 kya (RGFA) and (vi) old (older than 200 kya) gene flow (OGF). Admixture models (A & RGFA) reflect short episodes of genetic exchange which could have occurred in history of these species as suggested by the mtDNA data (Zieliński *et al.* 2013).

Following the analysis of two-population models, which favoured recent gene flow with demographic change, we wanted to check whether the same scenario of gene flow will be supported by more realistic three-population models. We thus built and compared three-population models analogous to M2, M3, M4 and M7 but allowing for a single demographic change in each population and gene flow not earlier than 200 kya (M2.VS.RGF, M3.VS.RGF, M4.VS.RGF and M7.VS.RGF, respectively).

Simulations and ABC analysis

Coalescent simulations were performed using FASTSIMCOAL2.01 (Excoffier *et al.* 2013). We simulated data using finite site mutation model (as our data did not fit the infinite site model) and single, fixed mutation rate. Loci were simulated as independent chromosomes. Special attention was paid to treat simulated data in exactly the same way as observed data. Thus, we simulated loci of the same lengths as in the observed ABC data set and used only biallelic sites for the calculation of summary statistics. We simulated exactly the same number of sequences as in the observed data set. The ABC analysis was performed within the ABCtoolbox (Wegmann *et al.* 2010), which facilitates the integration of simulations, summary statistics calculation, parameter estimation and validation.

Parameter values were sampled from uniform prior distributions, priors for population sizes were uniform on a log10 scale (Tables 1–3; S2–S3, Supporting information). Mutation rate ($\mu = 5.7 \times 10^{-9}$ per site, per generation) was calculated from the data, using nuclear sequences of *L. boscai* and *L. italicus* (Zieliński *et al.* 2014b), divergence time estimates from Pabijan *et al.* (2015) and generation time of 4 years (Nadachowska & Babik 2009). Recombination rate (r) prior spanned two orders of magnitude (1.0×10^{-10}–1.0×10^{-8} per generation between adjacent sites) and encompassed the mean value (6.0×10^{-9}, SD $\pm$ 2.50×10^{-9}) estimated

Table 1 Prior and posterior distribution of VS.RGF model for Lm – Lv. N_{anc}, N_{Lm}, N_{Lmanc}, NLv and N_{Lvanc} – population sizes of ancestral population, Lm, Lm before demographic change, Lv, Lv before demographic change, respectively. Nm – number of migrants per generation. T_S – time of split between species. T_{DLm} and T_{DLv} – time of demographic change in Lm and Lv, respectively. T_m – time of migration start. r – recombination rate between adjacent sites

	Prior*		Posterior characteristics						
					HPDI† 90		HPDI† 95		Posterior validation
Parameter	Minimum	Maximum	Mode	Mean	Lower	Upper	Lower	Upper	*P*-value‡
$\log_{10} N_{anc}$	4.5	6.7	5.06	5.19	4.52	5.76	4.52	5.92	**3.30E-09**
$\log_{10} N_{Lm}$	4.5	6.5	5.15	5.27	4.57	5.91	4.52	6.06	**6.39E-05**
$\log_{10} N_{Lmanc}$	4.5	6.5	4.97	5.28	4.52	6.03	4.52	6.23	**1.44E-05**
$\log_{10} N_{Lv}$	4.5	6.7	6.10	5.99	5.43	6.68	5.26	6.69	**1.11E-14**
$\log_{10} N_{Lvanc}$	4.5	6.7	5.72	5.64	4.78	6.53	4.68	6.63	5.11E-02
$Nm_{Lv\rightarrow Lm}$§	0.005	2	0.43	0.79	0.02	1.56	0.02	1.74	**1.09E-04**
$Nm_{Lm\rightarrow Lv}$¶	0.005	2	1.29	1.02	0.19	1.88	0.10	1.93	1.10E-01
T_{DLm}‖	1000	500 000	126 377	234 107	15 059	436 058	4761	459 996	**1.60E-09**
T_{DLv}‖	1000	500 000	296 889	263 546	63 361	476 177	40 289	491 222	6.21E-02
T_m‖	1	50 000	12 815	22 071	629	41 354	378	44 884	3.37E-01
T_S‖	50 000	2 500 000	936 461	1 071 020	268 834	1 853 650	171 438	2 013 700	**1.12E-07**
$r \times 10^{-9}$	0.1	10	4.33	5.05	0.84	9.28	0.51	9.63	1.89E-01

*All priors are uniformly distributed.
†Highest posterior density intervals.
‡*P*-values computed with Kolmogorov—Smirnoff test; bold values indicate significant deviations from uniformity after Bonferroni correction.
§$Nm_{Lv\rightarrow Lm}$ equals $m_{Lv\rightarrow Lm} \times N_{Lm}$
¶$Nm_{Lm\rightarrow Lv}$ equals $m_{Lm\rightarrow Lv} \times N_{Lv}$
‖All times given in generations.

Table 2 Prior and posterior distribution of VS.RGF model for Lm – LvIN. N_{anc}, N_{Lm}, N_{Lmanc}, N_{LvIN} and $N_{LvINanc}$ – population sizes of ancestral population, Lm, Lm before demographic change, LvIN, LvIN before demographic change, respectively. Nm – number of migrants per generation. T_S – time of split between species. T_{DLm} and T_{DLvIN} – time of demographic change in Lm and LvIN, respectively. T_m – time of migration start. r – recombination rate between adjacent sites

	Prior*		Posterior characteristics						
					HPDI† 90		HPDI† 95		Posterior validation
Parameter	Minimum	Maximum	Mode	Mean	Lower	Upper	Lower	Upper	*P*-value‡
$\log_{10} N_{anc}$	4.5	6.5	5.03	5.15	4.52	5.69	4.52	5.84	**7.08E-07**
$\log_{10} N_{Lm}$	4.5	6.5	5.27	5.38	4.68	6.10	4.59	6.22	**4.03E-06**
$\log_{10} N_{Lmanc}$	4.5	6.5	5.00	5.24	4.52	5.94	4.51	6.14	**2.20E-16**
$\log_{10} N_{LvIN}$	4.5	6.5	6.10	5.88	5.30	6.49	5.10	6.49	**1.09E-05**
$\log_{10} N_{LvINanc}$	4.5	6.5	5.63	5.57	4.84	6.38	4.74	6.46	2.85E-02
$Nm_{LvIN\rightarrow Lm}$§	0.005	2	0.44	0.78	0.02	1.54	0.02	1.72	**1.14E-08**
$Nm_{Lm\rightarrow LvIN}$¶	0.005	2	1.26	1.02	0.18	1.87	0.10	1.93	2.01E-02
T_{DLm}‖	1000	500 000	123 869	224 356	6209	421 013	4761	455 536	**3.35E-07**
T_{DLvIN}‖	1000	500 000	359 578	273 275	75 187	491 224	46 691	498 746	1.06E-01
T_m‖	1	50 000	12 312	21 351	378	40 311	378	44 323	4.92E-02
T_S‖	50 000	2 500 000	985 701	1 079 630	351 670	1 827 680	231 377	1 964 450	**9.22E-15**
$r \times 10^{-9}$	0.10	10	5.72	5.04	0.78	9.23	0.46	9.58	5.59E-02

*All priors are uniformly distributed.
†Highest posterior density intervals.
‡*P*-values computed with Kolmogorov–Smirnoff test; bold values indicate significant deviations from uniformity after Bonferroni correction.
§$Nm_{LvIN\rightarrow Lm}$ equals $m_{LvIN\rightarrow Lm}$ *x* N_{Lm}
¶$Nm_{Lm\rightarrow LvIN}$ equals $m_{Lm\rightarrow LvIN}$ *x* N_{LvIN}
‖All times given in generations.

with LDhat (McVean *et al.* 2002). For each model, we ran 2.0×10^5 exploratory simulations to examine whether the model was able to explain the observed data. Prior ranges were kept wide enough to cover biologically plausible ranges of parameter values, were identical and were adjusted for all models simultaneously, to avoid the risk of introducing bias into model selection by creating more and less optimized models. The final analyses were based on 10^6 data sets simulated under each demographic model. We retained 1% (10^4) best simulations for each model and computed the marginal likelihood of the observed and retained data sets under generalized linear models (GLM; Leuenberger & Wegmann 2010). We inspected posterior probability curves and the fraction of retained simulations with the marginal likelihood smaller or equal to that of the observed data (observed *P*-value) to determine whether models can faithfully reproduce the observed data. We assumed that *P*-values lower than 0.05 indicate that most of simulated data sets have higher likelihood than the likelihood of observed data; such models were excluded from the final model choice procedure. Error rate was controlled applying the Bonferroni correction. The best fitting model was selected via Bayes factors (ratios of model marginal densities).

Power estimation and posterior validation

For the three-population models, we applied the single model selection procedure, each within given temporal scenario of gene flow, whereas for the two-population models, both single and hierarchical model choice procedures were applied following Fagundes *et al.* (2007). In the hierarchical procedure, we first evaluated posterior probabilities of different demographic models nested within each scenario of gene flow and then compared best models among scenarios.

To estimate the power to distinguish between models, we generated for each model 1000 pseudo-observed data sets and checked how often the ABC model choice procedure correctly predicted the true model (the one that produced the data set). Each pseudo-observed data set was treated as the observed data and used to calculate marginal densities of all compared models. Bayes factors were then used to select the best model. As we were interested in the power to identify the true model overall as well as in the observed summary statistics

Table 3 Prior and posterior distribution of VS.RGF model for Lm – LvOUT. N_{anc}, N_{Lm}, N_{Lmanc}, N_{LvOUT} and $N_{LvOUTanc}$ – population sizes of ancestral population, Lm, Lm before demographic change, LvOUT, LvOUT before demographic change, respectively. Nm – number of migrants per generation. T_S – time of split between species. T_{DLm} and T_{DLvOUT} – time of demographic change in Lm and LvOUT, respectively. T_m – time of migration start. r – recombination rate between adjacent sites

	Prior*		Posterior characteristics						
					HPDI† 90		HPDI† 95		Posterior validation
Parameter	Minimum	Maximum	Mode	Mean	Lower	Upper	Lower	Upper	*P*-value‡
$\log_{10} N_{anc}$	4.5	6.5	5.07	5.17	4.53	5.71	4.52	5.85	**3.58E-04**
$\log_{10} N_{Lm}$	4.5	6.5	5.36	5.44	4.74	6.18	4.64	6.29	**2.12E-04**
$\log_{10} N_{Lmanc}$	4.5	6.5	5.00	5.23	4.52	5.93	4.51	6.13	**1.83E-11**
$\log_{10} N_{LvOUT}$	4.5	6.5	5.60	5.57	4.87	6.31	4.75	6.39	**1.15E-05**
$\log_{10} N_{LvOUTanc}$	4.5	6.5	5.27	5.39	4.55	6.12	4.52	6.26	**1.36E-04**
$Nm_{LvOUT\rightarrow Lm}$§	0.005	2	0.43	0.80	0.02	1.56	0.02	1.74	2.47E-02
$Nm_{Lm\rightarrow LvOUT}$¶	0.005	2	0.72	0.96	0.10	1.77	0.05	1.86	1.98E-01
T_{DLm}‖	1000	500 000	131 392	222 384	9777	422 081	4762	454 143	**5.73E-05**
T_{DLvOUT}‖	1000	500 000	234 201	251 382	49 897	464 184	29 003	481 193	5.37E-01
T_m‖	1	50 000	11 559	19 836	378	38 559	378	43 075	**1.05E-04**
T_S‖	50 000	2 500 000	1 059 700	1 115 540	425 717	1 820 070	327 234	1 964 400	**1.23E-09**
$r \times 10^{-9}$	0.10	10	6.17	5.09	0.92	9.35	0.52	9.63	5.94E-03

*All priors are uniformly distributed.
†Highest posterior density intervals.
‡*P*-values computed with Kolmogorov–Smirnoff test; bold values indicate significant deviations from uniformity after Bonferroni correction.
§$Nm_{LvOUT\rightarrow Lm}$ equals $m_{LvOUT\rightarrow Lm} \times N_{Lm}$
¶$Nm_{Lm\rightarrow LvOUT}$ equals $m_{Lm\rightarrow LvOUT} \times N_{LvOUT}$
‖All times given in generations.

space, separate analyses were performed using the pseudo-observed data sets drawn from all or from retained simulations.

We checked for a bias in the posterior distributions by generating 1000 pseudo-observed data sets with known parameter values and computed coverage property of the posterior distributions obtained with ABC-GLM regression adjustment. If the parameter values for these pseudo-observed data were randomly chosen from the prior distribution, we expect the posterior quantiles (the position of the true values within the posterior distribution) to be uniformly distributed. The uniformity of the posterior quantiles for each parameter was checked with a Kolmogorov–Smirnoff test and its significance was obtained after the Bonferroni correction.

Results

Polymorphism and differentiation

The full poly data set comprised alignments of 74 genes of the average length of 499 bp (total length 36 918 bp) acquired from 39 Lm and 45 Lv individuals (31 and 38 populations, respectively), sequenced to the average per base coverage of 1017 ± (SD) 1181. Physical phasing using information contained in the overlapping Illumina reads resulted in phase-resolved haplotypes (alleles) for most (95.1%) heterozygous genotypes. In the remaining 4.9% cases, phasing was incomplete and haplotypes were resolved randomly. As no test of linkage disequilibrium was significant at the FDR level 0.05, we further consider the markers unlinked. Species-wide nucleotide diversity was almost twice as high in Lv as in Lm ($\pi_{Lv} = 0.0101 \pm 0.0071$, $\pi_{Lm} = 0.0057 \pm 0.0050$, Wilcoxon test, $T = 38$, $P < 10^{-6}$, Table S4, Supporting information). Also, within-population diversity was significantly higher in Lv ($\pi_{Lv} = 0.0063$, $\pi_{Lm} = 0.0041$, Mann–Whitney *U*-test, $Z = 6.42$, $P < 10^{-6}$, Fig. S3, Table S5, Supporting information). Between-population nucleotide distance was also higher in Lv (mean $d_{XYLv} = 0.0103$, $d_{XYLm} = 0.0055$, Mann–Whitney *U*-test, $Z = 27.70$, $P < 10^{-6}$, Fig. S3, Table S5, Supporting information).

Interspecific F_{ST} of 0.50 was highly significant ($P < 0.0001$). The mean F_{ST} between interspecific population pairs was 0.66 ± 0.05 (Table S6 and Fig. S4, Supporting information). Within-species differentiation was substantial, but weaker in Lm ($F_{ST} = 0.22$), than in Lv ($F_{ST} = 0.34$) (Table S6 and Fig. S4, Supporting

information). The Structure analysis robustly identified three genetic clusters and little admixture between them, that is, in most populations, all individuals were classified entirely or almost entirely to a single cluster (Fig. 1). There was no indication of additional, lower level structuring within the data set (Fig. S5, Supporting information). All Lm populations formed a single cluster while two clusters were identified in Lv, one grouping populations within the Carpathian basin and the other those outside the Carpathian belt (LvIN and LvOUT, respectively). Only two Lv populations (68 & 69) were highly admixed (admixture > 30%), and these were not included in the ABC data set. The mean F_{ST} between pairs of LvIN and LvOUT populations was high (0.50), whereas pairwise F_{ST} within groups was lower, 0.30 for LvIN and 0.17 for LvOUT (Table S6, Supporting information). Tajima's D was significantly negative for both species ($P < 0.001$), more so in Lv ($D_{Lv} = -1.13 \pm 0.69$ vs. $D_{Lm} = -0.92 \pm 0.83$, Wilcoxon test, $T = 1087$, $P = 0.11$, Table S4, Supporting information).

The ABC data set included 66 markers of the average length of 484 bp (31 929 bp) and consisted of one gene copy per marker sampled from each of 26 Lm and 32 Lv populations (Tables S7–S8, Supporting information). Among 2046 polymorphic sites (S), 231 (11.29%) were shared between species (SS) and 52 (2.54%) were fixed differences (SF). Many more polymorphisms were private (SP) to Lv (1330; 65%) than to Lm (433; 21.16%).

Model choice

The *P*-values calculated under the GLM were used to check whether tested models were able to reproduce the observed data. For five of seven-three-population models (M1, M2, M3, M5 and M6), the observed data fell well into the distribution of retained simulated data (Table S9, Supporting information) and these models were used for model choice. The best model was the M3, with posterior probability (PP) 0.80 (Table S9, Supporting information); this model allowed migration between LvIN and LvOUT as well as between LvIN and Lm. The second best model (M5), which allowed migration only between Lm and LvIN, also obtained substantial support (PP = 0.18). The overall power to correctly predict the true model ranged from 0.60 for M1 to 0.97 for M3 (mean = 0.77, Table S10, Supporting information). The power, however, decreased in the observed summary statistics space where it ranged from 0.42 for M5 to 0.68 for M2 (mean = 0.50), but for all models, it was higher than the random expectation of 0.2 (Table S11, Supporting information).

All two-population models were able to reproduce the observed data (Table 4). Within each gene flow scenario, the VS models always outperformed the CS models (Table 4). The VS.RGF model had the highest PP for each population pair, although in the LvIN-LvOUT comparison, its PP was below 0.5 (Table 4). The second best in all interspecific comparisons was the RGFA model, while in the LvIN-LvOUT comparison, the CGF and RGFA models performed similarly (Table 4). The power to correctly predict the true model was similar in all interspecific comparisons (0.40–0.42); in all cases except VS.NGF, the power was higher than the random expectation of 0.17 (Table S12, Supporting information). In all cases, the lowest overall power was found for the VS.NGF and VS.RGF as simulations produced by these models were commonly choosing as true models the VS.OGF and VS.CGF, respectively (Table S12, Supporting information). However, VS.RGF model gained power in the observed summary statistics space where it increased to 0.66 (Table S13, Supporting information).

Each two-population model including Lm involved comparison of nonsister groups. Because models not considering genetic exchange with the third closely related population may give biased parameter estimates, we additionally performed model selection and power analysis for more realistic three-population models allowing for demographic change and recent gene flow. The M4.VS.RGF model, assuming recent gene flow between both Lv groups as well as between Lm and LvOUT, obtained the highest posterior probability (Table S14, Supporting information). However, also the other two models that allowed migration between Lm and LvIN (M3.VS.RGF) or between Lm and both Lv groups (M7.VS.RGF) had considerable support (Table S14, Supporting information). The overall power to correctly predict the true model ranged from 0.45 for M4.VS.RGF to 0.75 for M2.VS.RGF (mean = 0.58), and for all models, it was higher than the random expectation of 0.25 (Table S15, Supporting information). Nevertheless, power analysis conducted within the observed summary statistics space showed that the results of model choice could be positively misleading: simulations generated by two other models assuming gene flow between Lm and Lv (M3.VS.RGF and M7.VS.RGF) more often favoured M4.VS.RGF model than models, which produced them (Table S16, Supporting information). Thus, we conclude that there was not enough resolution in the data to evaluate complex three-population models allowing temporal changes in gene flow and demography.

History of divergence and gene flow

The three-population model M3 indicates the Messinian (6.3 mya) divergence between Lm and Lv and the

Table 4 Performance of two-population models

	LM_LV			LM_LVIN			LM_LVOUT			LVIN_LVOUT		
Model	*P*	PP	PP_h	*P*	PP	PP_h	*P*	PP	PP_h	*P*	PP	PP_h
CS.NGF	0.898	0.003	—	0.831	0.001	—	0.950	0.003	—	0.981	0.001	—
CS.CGF	0.009	0.000	—	0.013	0.000	—	0.012	0.000	—	0.782	0.005	—
CS.RGF	0.999	0.081	—	0.969	0.036	—	0.984	0.071	—	1.000	0.035	—
CS.A	0.519	0.001	—	0.809	0.001	—	0.731	0.000	—	0.662	0.000	—
CS.OGF	0.954	0.002	—	0.959	0.001	—	0.959	0.001	—	0.992	0.000	—
VS.NGF	0.140	0.022	0.024	0.255	0.029	0.030	0.146	0.010	0.011	0.694	0.013	0.013
VS.CGF	0.034	0.030	0.033	0.229	0.039	0.041	0.041	0.010	0.011	0.961	0.261	0.273
VS.RGF	1.000	0.620	0.681	1.000	0.598	0.624	1.000	0.703	0.761	0.999	0.431	0.450
VS.A	0.823	0.047	0.051	0.877	0.045	0.047	0.891	0.014	0.015	0.895	0.012	0.013
VS.RGFA	0.997	0.162	0.178	1.000	0.184	0.192	0.999	0.165	0.179	0.986	0.222	0.232
VS.OGF	0.126	0.030	0.033	0.315	0.064	0.067	0.197	0.021	0.023	0.648	0.018	0.019

P — fraction of retained simulations with the marginal likelihood smaller or equal to that of the observed data. PP — posterior probability calculated when all models compared simultaneously. PP_h — posterior probability calculated within hierarchical model selection procedure.

Pleistocene (1.0 mya) divergence between LvIN and LvOUT (Fig. S6, Table S2 and Fig. S7, Supporting information). For estimated effective population size (*Ne*) of LvIN, 4.64 million (m) was an order of magnitude higher than that of LvOUT (0.34 m) and two orders of magnitude higher than that of Lm (0.06 m). According to the posterior validation (Fig. S8, Table S2, Supporting information) and posterior probability curves (Fig. S7, Supporting information), LvIN *Ne* is underestimated. However, when compared with two-population models, it appears severely overestimated. Both ancestral populations had similar *Ne* of ca. 0.10 m (Table S2, Supporting information). Moderately strong and asymmetric gene exchange between LvIN and both Lm and LvOUT was inferred. Intraspecific migration rate was an order of magnitude stronger from LvIN to LvOUT ($m_{LvIN\ to\ LvOUT}$ $1.8*10^{-06}$ vs. $m_{LvOUT\ to\ LvIN}$ $3.4*10^{-07}$). Interspecific migration was two orders of magnitude stronger from LvIN to Lm than in the opposite direction ($m_{LvIN\ to\ Lm}$ $6.5*10^{-06}$ vs. $m_{Lm\ to\ LvIN}$ $8.3*10^{-08}$). Interestingly, interspecific migration rate from LvIN to Lm appears at least three times higher than migration within Lv (Table S2, Supporting information).

The two-population models involving various population pairs consistently estimated the time of divergence between Lm and Lv as 3.7 to 4.2 mya (Fig. 3). The divergence between LvIN and LvOUT was estimated at ca. 3.0 mya (Fig. S9, Supporting information). Thus, interspecific divergence is younger and intraspecific divergence is considerably older than estimates from the three-population model. Demographic expansions were detected in all groups (Figs 3, S9 and Tables 1–3, S3, Supporting information). In Lm, the twofold expansion occurred ca. 0.5 mya leading to the current *Ne* of 0.14–0.23 m (Tables 1–3 and Fig. 3). The two- or threefold demographic expansions in LvIN and LvOUT occurred earlier, 0.9–1.5 mya (Tables 2–3 and S3, Supporting information). The current *Ne* of LvIN (ca. 1.09–1.25 m) is three to four times higher than LvOUT (ca. 0.26–0.39 m, Tables 2–3, S3 and Figs 3b,c, S9, Supporting information). All interspecific models clearly support recent (starting 45–52 kya) gene flow. The model comparing Lm and Lv (LvIN an LvOUT combined) indicated three times higher migration rate from Lv to Lm than in the opposite direction ($m_{Lv\ to\ Lm}$ $3.0*10^{-06}$ vs. $m_{Lm\ to\ Lv}$ $1.0*10^{-06}$) (Fig. 3a, Table 1 and Fig. S10, Supporting information). Patterns of gene flow between Lm and each Lv group differed. The rate of gene flow between Lm and LvOUT was similar in both directions ($m_{LvOUT\ to\ Lm}$ $1.8*10^{-06}$ vs. $m_{Lm\ to\ LvOUT}$ $1.8*10^{-06}$) (Fig. 3c, Table 3 and Fig. S11, Supporting information). On the contrary gene flow between Lm and LvIN was asymmetric, with migration rate two times higher from LvIN to Lm ($m_{LvIN\ to\ Lm}$ $2.3*10^{-06}$ compared to $m_{Lm\ to\ LvIN}$ $1.00*10^{-06}$, Fig. 3b, Table 2, Fig. S12, Supporting information). Gene exchange between smooth newt groups started ca. 130 kya and was also asymmetric ($m_{LvIN\ to\ LvOUT}$ $3.3*10^{-06}$ compared to $m_{LvOUT\ to\ LvIN}$ $1.3*10^{-06}$, Fig. S9, Table S3, Fig. S13, Supporting information). Gene flow is also given as the number of migrants per generation (Nm, Figs 3, S6, S9 and Table 1–3, S2-S3, Supporting information), that is the product of *Ne* and migration rate. To check whether the marginal posterior distributions estimated from the best models were biased, we generated 1000 pseudo-observed data sets for each best model and tested uniformity of posterior quantile distributions for each parameter. According to the

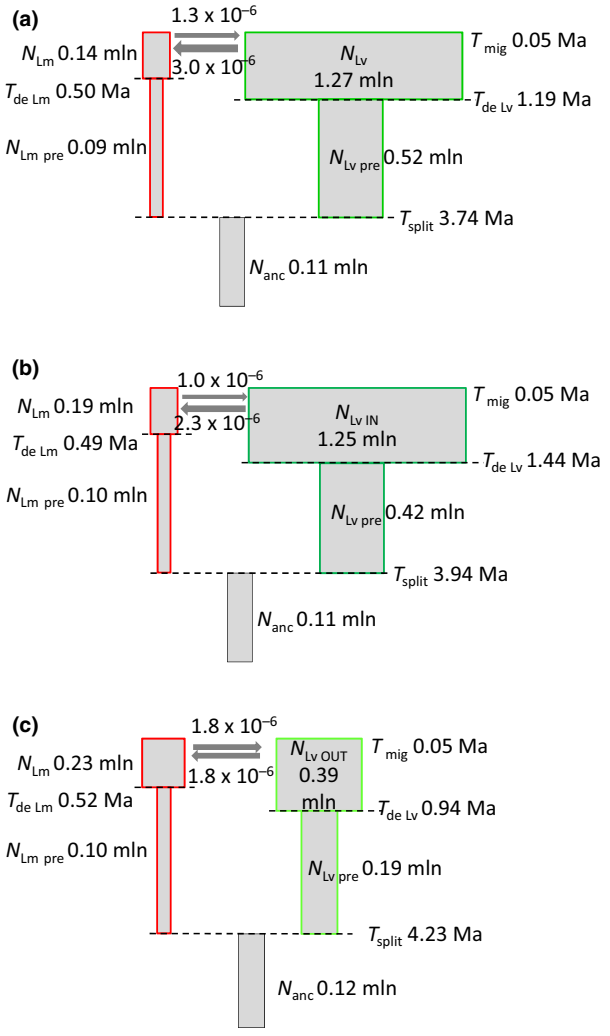

Fig. 3 Parameters estimated from best two-group model – VS.RGF (demographic change and recent migration). (a) Lm – Lv (combined LvIN and LvOUT), (b) Lm – LvIN, (c) Lm – LvOUT. N_{Lm}, N_{Lv}, N_{LvIN} and N_{LvOUT} – population size of Lm, Lv, LvIN and LvOUT, respectively; N_{anc} ancestral population size. N_{Lmpre}, N_{Lvpre} – population size before size change of Lm and given Lv group, respectively. T_{split} – time of split. T_{deLm} and T_{deLv} – time of demographic change in Lm and given Lv group, respectively. T_{mig} – time of migration start. Numbers above and below arrows indicate migration rates.

Kolmogorov–Smirnoff test results (Table 1–3, S2-S3, Supporting information) in each best model, some parameters were biased. However, visual inspection of the distributions of posterior quantiles (Figs S7, S14-S17, Supporting information) suggests that most deviations from uniformity were slight. In certain models, the true values of some parameters were more often found in the centre of the distribution, which is the consequence of overly wide priors. This kind of bias does not affect interpretation of posterior distributions and may only slightly decrease precision of the estimates.

Discussion

Demographic history of the Carpathian and smooth newts

The divergence of the Carpathian (Lm) and smooth (Lv) newts has been characterized by prolonged isolation followed by a recent secondary contact between all population groups. Species divergence was dated between the upper Miocene (6.3 mya; 95% HDPI 1.65–9.98 mya) and middle Pliocene (3.7–4.2 mya; 95% HDPI 0.68–8.05 mya). These estimates are plausible as fossils uncontroversially assigned to both species are known from the upper Pliocene (Roček 1994; Pabijan *et al.* 2015). As the original Lm mtDNA was replaced by Lv mtDNA, we cannot estimate the time of divergence from mtDNA (Babik *et al.* 2005; Zieliński *et al.* 2013). Although the credibility intervals of divergence from three- and two-population models overlap, it appears that the three-population models allowing constant gene flow may overestimate the time of divergence. Posteriors of the divergence time are much flatter in these models, and, as evidenced by the two-population models, constant gene flow is unlikely in this system. A given amount of shared polymorphism may be explained either by long divergence and substantial gene flow or by more recent divergence and limited or no gene flow (Nielsen & Wakeley 2001). Therefore, models assuming constant gene flow tend to overestimate the divergence time. In three-population model allowing for demographic change and recent gene flow, the time of divergence was estimated at ca. 4.2 mya (95% HDPI 0.69–8.35 mya). In each case, interspecific genetic differentiation predates the Pleistocene glaciations. This pattern is repeatedly found in temperate amphibians (Weisrock *et al.* 2001; Wielstra & Arntzen 2011; Pabijan *et al.* 2013). Perhaps speculations about the role of environmental factors in initiating divergence are premature, but we note that our divergence time estimates fall around the time of the Messinian salinity crisis, a major climatic and environmental event in Europe (Krijgsman *et al.* 1999). Upper Pliocene (3.0 mya; 95% HDPI 0.62–6.41 mya) or Pleistocene (1.0 mya; 95% HDPI 0.21–2.83 mya) estimates of intraspecific divergence between the Lv groups are consistent with those between the major mtDNA lineages present in both groups (Babik *et al.* 2005; Pabijan *et al.* 2015). Thus, climatic oscillations during the Pleistocene could trigger intraspecific differentiation within Lv. The Pleistocene climatic changes affected most species inhabiting temperate regions by causing range shifts and long-term range fragmentation (Hewitt 2000, 2004). Long-term geographical isolation could facilitate intraspecific genetic differentiation.

As our primary focus was on gene flow rather than on demography, our models allow for only a single, instantaneous demographic change as an approximation

of complex historical demography. Changes of population size inferred from the two-population models suggest that since initial divergence, populations of both species at least doubled reaching the current sizes of approximately two hundred thousand and over one million in case of Lm and Lv, respectively. Interpretation of the estimated *Ne* values is not straightforward because the relationship between the census size and *Ne* is not obvious in our case. We use the coalescent *Ne*, which is an inverse of the coalescent rate (Nordborg & Krone 2002; Sjödin *et al.* 2005). If one gene copy is sampled per deme in the many deme model, the *Ne* in the collecting phase is estimated (Wakeley 2009). In this model, *Ne* is often larger than census population size and is determined mainly by the rate of migration between demes (Wakeley 2009), which remains unknown. Lv population size could be also overestimated due to migration from surrounding, unsampled, Lv lineages (Beerli 2004). This is especially likely for LvIN, which has been exchanging genes with Lv populations from southern Europe (M. Pabijan *et al.* submitted).

History of genetic exchange between the evolutionary lineages

The roles of hybridization and interspecific gene flow in speciation are controversial and remain poorly understood (Coyne & Orr 2004; Abbott *et al.* 2013; Harrison & Larson 2014; Seehausen *et al.* 2014). The pattern of contemporary hybridization is only a single snapshot of a complex historical process (Abbott *et al.* 2013). Thus, to understand the process of divergence, a longer-scale perspective on historical gene flow between species is essential (Sousa & Hey 2013). We found evidence for recent (last glacial period) gene flow between Lm and Lv despite their relatively old divergence (4–6 mya) and presumably long periods of isolation. The massive mitochondrial introgression, resulting in complete mtDNA replacement (Zieliński *et al.* 2013), was thus at least to some extent accompanied by nuclear gene flow. Introgression of two major mtDNA lineages, G and J, was dated to < 100 kya (Zieliński *et al.* 2013), consistent with our results for the nuclear data.

The models used in this study almost certainly oversimplify the complexity of historical genetic exchange in this system. For example, the model allowing both recent gene flow and more ancient admixture also received substantial support and multiple periods of genetic exchange are suggested by the presence in Lm of the mtDNA lineage I, a likely remnant of an ancient introgression (Babik *et al.* 2005; Zieliński *et al.* 2013; Pabijan *et al.* 2015). A model of secondary contact but with a much longer period of genetic exchange spanning the entire Pleistocene received the highest support in the transcriptome resequencing study of Stuglik & Babik (*in press*). The most complex scenarios assuming temporal changes in demography and gene flow were analysed in two-population models. Each of such models involving Lm excluded one group of Lv and thus oversimplified the biological reality. Gene flow from not sampled (or not included in the model) populations may affect both the estimates of population sizes and gene flow (Beerli 2004; Slatkin 2005; Strasburg & Rieseberg 2010). Unfortunately, there was not enough power in our data to meaningfully analyse three-population models with variable demography and migration. More extensive data, preferably from long continuous genomic fragments and utilizing haplotype information, should allow analysis of such complex models in the future. Thus, while some uncertainty about the details of historical gene flow remains, a long period of isolation followed by period(s) of genetic exchange between Lm and Lv appears robustly supported by the data.

Nevertheless, it may seem surprising that populations so divergent with respect to morphology, behaviour and ecology still maintain the ability to exchange genes, despite apparently strong prezygotic isolation (Babik *et al.* 2003). Strong reproductive isolation should result in very low per generation migration rates (m) between the two species (Sambatti *et al.* 2012). Thus, low migration rates (ca. 10^{-6} per gene copy per generation) estimated in this study are fully consistent with strong assortative mating observed in the hybrid zone and population genetic studies, which found little evidence for contemporary gene flow between the species (Zieliński *et al.* 2013, 2014a). However, due to the large effective population sizes, these low migration rates translate into a relatively high number of effective migrants (Nm = 0.39–1.29). Both theory (Wright 1931) and empirical studies (Sambatti *et al.* 2012) indicate that if populations are large, even a low rate of gene flow can prevent genetic differentiation due to drift. Thus, the large population sizes of the two hybridizing species have two main consequences. First, a relatively low rate of gene flow is needed to prevent their differentiation at neutral loci. Second, the efficacy of selection relative to genetic drift in generating divergence is increased so we suspect that the observed differentiation can in large part be attributed to selection. On the other hand, efficient selection may facilitate the spread of universally beneficial alleles originating in either species, so that even a low amount of gene flow may allow species to share adaptations (Morjan & Rieseberg 2004).

Both the three- and two-population models support asymmetric nuclear gene flow. Introgression between hybridizing species is often asymmetric for reasons that are not fully understood (Barton & Hewitt 1985; Orive

& Barton 2002; Niemiller *et al.* 2008). In newts, long-term asymmetry is driven by a higher rate of gene flow from LvIN to both Lm and LvOUT, which is consistent with the observed admixture of Lv genes in several Lm populations adjacent to the Carpathian basin (Zieliński *et al.* 2014a). This pattern could be explained by expansion-related phenomena (Currat *et al.* 2008; Excoffier *et al.* 2009) or by intraspecific polymorphism in reproductive incompatibilities (Cutter 2012). Under the scenario modelled by Currat *et al.* (2008), neutral introgression from the resident to the invading population is expected. Invasion of Lm into the Lv range has previously been invoked to explain mtDNA replacement (Zieliński *et al.* 2013). Explanation of the geographically variable asymmetry in nuclear introgression would require expansion of Lm, and possibly also LvOUT into the LvIN-inhabited areas, but weaker or no expansion of Lm into the LvOUT range. Potentially, the observed asymmetry may also reflect differences in the time since secondary contact between Lm and the two lineages of Lv. This possibility could be evaluated by using information contained in haplotype spectra to estimate the time of secondary contact more precisely (Harris & Nielsen 2013). Genomic heterogeneity in the pattern of gene flow between Lm and Lv inferred from the site frequency spectrum (Stuglik & Babik *in press*) argues against the invasion-related neutral explanation. This is because asymmetric gene flow was found only in the portion of the genome characterized by a low migration rate, where selection may oppose introgression. No asymmetry was detected in the more freely introgressing fraction of the genome, which would be expected if neutral invasion-related phenomena were involved. A second explanation for geographical variation in the patterns of asymmetry involves intraspecific polymorphism in reproductive isolation between species. The genetic architecture of isolation between a pair of taxa may vary spatially due to environmental, ecological or genetic variation in factors that contribute to isolation (Nolte *et al.* 2009; Teeter *et al.* 2010). Several recent studies demonstrate substantial intraspecific polymorphism for hybrid incompatibilities (Sweigart *et al.* 2007; Good *et al.* 2008; Corbett-Detig *et al.* 2013; Charron *et al.* 2014). Introgression may be easier between some genetic groups if their genomes harbour fewer incompatible alleles and thus intrinsic selection against hybrids is weaker (Cutter 2012). Hence, the differences in the pattern of gene flow between Lm and two Lv groups may suggest regional differences in the genetic architecture of isolation between the species. The relevance of such polymorphism to the process of speciation is of great interest and has been the focus of much debate (Cutter 2012). Further insights may be obtained by comparing introgression between multiple transects through Lm/Lv hybrid zones. If the architecture of reproductive isolation differs between Lm and the two Lv lineages, then similar patterns of introgression are expected between transects involving the same Lv lineage, but transects involving various lineages should consistently differ (Teeter *et al.* 2010; Cutter 2012; Seehausen *et al.* 2014).

Conclusions

This study provided quantitative, model-based insight into the history of divergence and a longer-scale perspective on genetic exchange between the Carpathian and smooth newts. Despite introgression of nuclear genes, which followed period(s) of isolation, the species have maintained their distinctiveness, which suggests that gene flow has not affected genomic regions responsible for species-specific adaptations. The Carpathian newt hybridizes with two evolutionary lineages of the smooth newt, exchanging genes symmetrically with one of them but asymmetrically with the other. We argue that intraspecific polymorphism for hybrid incompatibilities segregating within the smooth newt could explain this pattern; this hypothesis can be tested in replicated hybrid zones. The results of our study highlight the importance of incorporating intraspecific genetic structure into the models investigating the history of divergence.

Acknowledgements

We thank M. Bonk, M. Chloupek, D. Cogălniceanu, S-D. Covaciu-Marcov, M. Herdegen, M. Liana, Z. Prokop, J. Radwan and M. Stuglik for help in sampling. We are grateful to Daniel Wegmann for providing updates to the ABCtoolbox and discussions on the ABC approach. Special thanks for Jochen Wolf and his group for discussion on the project and their hospitality during P.Z.'s internship at the Evolutionary Biology Centre, Uppsala University. The work was supported by the Polish National Science Center grant No. 8171/B/P01/2011/40 to WB and by Jagiellonian University grants, DS/WBiNoZ/INoS/762/14, DS/MND/WBiNoZ/INoŚ/36/2013. The study was performed with the financial support of the Foundation for Polish Science.

References

Abbott R, Albach D, Ansell S *et al.* (2013) Hybridization and speciation. *Journal of Evolutionary Biology*, **26**, 229–246.

Aeschbacher S, Futschik A, Beaumont MA (2013) Approximate Bayesian computation for modular inference problems with many parameters: the example of migration rates. *Molecular Ecology*, **22**, 987–1002.

Babik W, Rafiński J (2004) Relationship between morphometric and genetic variation in pure and hybrid populations of the smooth and Montandon's newt (*Triturus vulgaris* and *T. montandoni*). *Journal of Zoology*, **262**, 135–143.

Babik W, Szymura JM, Rafiński J (2003) Nuclear markers, mitochondrial DNA and male secondary sexual traits variation in a newt hybrid zone (*Triturus vulgaris* x *T. montandoni*). *Molecular Ecology*, **12**, 1913–1930.

Babik W, Branicki W, Crnobrnja-Isailović J *et al.* (2005) Phylogeography of two European newt species – discordance between mtDNA and morphology. *Molecular Ecology*, **14**, 2475–2491.

Barton N, Bengtsson BO (1986) The barrier to genetic exchange between hybridising populations. *Heredity*, **57**, 357–376.

Barton NH, Hewitt GM (1985) Analysis of hybrid zones. *Annual Review of Ecology and Systematics.*, **16**, 113–148.

Bateson W (1909) *Mendel's Principles of Heredity*. Cambridge University Press, Cambridge.

Beaumont MA, Zhang W, Balding DJ (2002) Approximate Bayesian computation in population genetics. *Genetics*, **162**, 2025–2035.

Beerli P (2004) Effect of unsampled populations on the estimation of population sizes and migration rates between sampled populations. *Molecular Ecology*, **13**, 827–836.

Bertorelle G, Benazzo A, Mona S (2010) ABC as a flexible framework to estimate demography over space and time: some cons, many pros. *Molecular Ecology*, **19**, 2609–2625.

Boulesteix AL, Strimmer K (2007) Partial least squares: a versatile tool for the analysis of high-dimensional genomic data. *Briefings in Bioinformatics*, **8**, 32–44.

Charron G, Leducq JB, Landry CR (2014) Chromosomal variation segregates within incipient species and correlates with reproductive isolation. *Molecular Ecology*, **23**, 4362–4372.

Chikhi L, Sousa VC, Luisi P, Goossens B, Beaumont MA (2010) The confounding effects of population structure, genetic diversity and the sampling scheme on the detection and quantification of population size changes. *Genetics*, **186**, 983–995.

Corbett-Detig RB, Zhou J, Clark AG, Hartl DL, Ayroles JF (2013) Genetic incompatibilities are widespread within species. *Nature*, **504**, 135–137.

Coyne JA, Orr HA (2004) *Speciation*. Sinauer, Sunderland.

Csillery K, Blum MGB, Gaggiotti OE, Francois O (2010) Approximate Bayesian Computation (ABC) in practice. *Trends in Ecology and Evolution*, **25**, 410–418.

Currat M, Ruedi M, Petit RJ, Excoffier L (2008) The hidden side of invasions: massive introgression by local genes. *Evolution*, **62**, 1908–1920.

Cutter AD (2012) The polymorphic prelude to Bateson–Dobzhansky–Muller incompatibilities. *Trends in Ecology & Evolution*, **27**, 209–218.

Dobzhansky T (1936) Studies on hybrid sterility. II. Localization of sterility factors in *Drosophila Pseudoobscura* hybrids. *Genetics*, **21**, 113–135.

Earl DA, vonHoldt BM (2012) STRUCTURE HARVESTER: a website and program for visualizing STRUCTURE output and implementing the Evanno method. *Conservation Genetics Resources*, **4**, 359–361.

Edwards S, Beerli P (2000) Perspective: gene divergence, population divergence, and the variance in coalescence time in phylogeographic studies. *Evolution*, **54**, 1839–1854.

Evanno G, Regnaut S, Goudet J (2005) Detecting the number of clusters of individuals using the software STRUCTURE: a simulation study. *Molecular Ecology*, **14**, 2611–2620.

Excoffier L, Lischer HEL (2010) Arlequin suite ver 3.5: a new series of programs to perform population genetics analyses under Linux and Windows. *Molecular Ecology Resources*, **10**, 564–567.

Excoffier L, Foll M, Petit RJ (2009) Genetic consequences of range expansions. *Annual Review of Ecology, Evolution, and Systematics*, **40**, 481–501.

Excoffier L, Dupanloup I, Huerta-Sánchez E, Sousa VC, Foll M (2013) Robust demographic inference from genomic and SNP data. *PLoS Genetics*, **9**, e1003905.

Fagundes NJR, Ray N, Beaumont M *et al.* (2007) Statistical evaluation of alternative models of human evolution. *Proceedings of the National Academy of Sciences of the United States of America*, **104**, 17614–17619.

Falush D, Stephens M, Pritchard JK (2007) Inference of population structure using multilocus genotype data: dominant markers and null alleles. *Molecular Ecology Notes*, **7**, 574–578.

Feder JL, Egan SP, Nosil P (2012) The genomics of speciation-with-gene-flow. *Trends in Genetics*, **28**, 342–350.

Good JM, Handel MA, Nachman MW (2008) Asymmetry and polymorphism of hybrid male sterility during the early stages of speciation in house mice. *Evolution*, **62**, 50–65.

Harris K, Nielsen R (2013) Inferring demographic history from a spectrum of shared haplotype lengths. *PLoS Genetics*, **9**, e1003521.

Harrison RG, Larson EL (2014) Hybridization, introgression, and the nature of species boundaries. *Journal of Heredity*, **105**, 795–809.

Hewitt G (2000) The genetic legacy of the quaternary ice ages. *Nature*, **405**, 907–913.

Hewitt GM (2004) Genetic consequences of climatic oscillations in the Quaternary. *Philosophical Transactions of the Royal Society B: Biological Sciences*, **359**, 183–195.

Hewitt GM (2011) Quaternary phylogeography: the roots of hybrid zones. *Genetica*, **139**, 617–638.

Hoffmann AA, Sgro CM (2011) Climate change and evolutionary adaptation. *Nature*, **470**, 479–485.

Hubisz MJ, Falush D, Stephens M, Pritchard JK (2009) Inferring weak population structure with the assistance of sample group information. *Molecular Ecology Resources*, **9**, 1322–1332.

Joyce P, Marjoram P (2008) Approximately sufficient statistics and bayesian computation. *Statistical Applications in Genetics and Molecular Biology*, **7**, 26.

Krijgsman W, Hilgen FJ, Raffi I, Sierro FJ, Wilson DS (1999) Chronology, causes and progression of the Messinian salinity crisis. *Nature*, **400**, 652–655.

Kronforst MR, Hansen MEB, Crawford NG *et al.* (2013) Hybridization reveals the evolving genomic architecture of speciation. *Cell Reports*, **5**, 666–677.

Leuenberger C, Wegmann D (2010) Bayesian computation and model selection without likelihoods. *Genetics*, **184**, 243–252.

Mallet J (2005) Hybridization as an invasion of the genome. *Trends in Ecology and Evolution*, **20**, 229–237.

Mallet J (2007) Hybrid speciation. *Nature*, **446**, 279–283.

McVean G, Awadalla P, Fearnhead P (2002) A coalescent-based method for detecting and estimating recombination from gene sequences. *Genetics*, **160**, 1231–1241.

Morjan CL, Rieseberg LH (2004) How species evolve collectively: Implications of gene flow and selection for the spread of advantageous alleles. *Molecular Ecology*, **13**, 1341–1356.

Muller HJ, Pontecorvo G (1942) Recessive genes causing interspecific sterility and other disharmonies between *Drosophila melanogaster* and *simulans*. *Genetics*, **27**, 157.

Nadachowska K, Babik W (2009) Divergence in the face of gene flow: the case of two newts (Amphibia: salamandridae). *Molecular Biology and Evolution*, **26**, 829–841.

Nadachowska-Brzyska K, Zieliński P, Radwan J, Babik W (2012) Interspecific hybridization increases MHC class II diversity in two sister species of newts. *Molecular Ecology*, **21**, 887–906.

Nadachowska-Brzyska K, Burri R, Olason PI *et al.* (2013) Demographic divergence history of pied flycatcher and collared flycatcher inferred from whole-genome re-sequencing data. *PLoS Genetics*, **9**, e1003942.

Nei M, Kumar S (2000) *Molecular Evolution and Phylogenetics*. Oxford University Press, New York.

Nei M, Li WH (1979) Mathematical model for studying genetic variation in terms of restriction endonucleases. *Proceedings of the National Academy of Sciences of the United States of America*, **76**, 5269–5273.

Nielsen R, Wakeley J (2001) Distinguishing migration from isolation: a Markov chain Monte Carlo approach. *Genetics*, **158**, 885–896.

Niemiller ML, Fitzpatrick BM, Miller BT (2008) Recent divergence with gene flow in Tennessee cave salamanders (Plethodontidae: *Gyrinophilus*) inferred from gene genealogies. *Molecular Ecology*, **17**, 2258–2275.

Nolte AW, Gompert Z, Buerkle CA (2009) Variable patterns of introgression in two sculpin hybrid zones suggest that genomic isolation differs among populations. *Molecular Ecology*, **18**, 2615–2627.

Nordborg M, Krone SM (2002) Separation of time scales and convergence to the coalescent in structured populations. In: *Modern Developments in Theoretical Population Genetics*, pp. 194–232. The Legacy of Gustave Malecot. Oxford University Press, Oxford.

Nosil P (2008) Speciation with gene flow could be common. *Molecular Ecology*, **17**, 2103–2106.

Nosil P, Egan SP, Funk DJ (2008) Heterogeneous genomic differentiation between walking-stick ecotypes: "Isolation by adaptation" and multiple roles for divergent selection. *Evolution*, **62**, 316–336.

Orive ME, Barton NH (2002) Associations between cytoplasmic and nuclear loci in hybridizing populations. *Genetics*, **162**, 1469–1485.

Pabijan M, Wandycz A, Hofman S *et al.* (2013) Complete mitochondrial genomes resolve phylogenetic relationships within *Bombina* (Anura: Bombinatoridae). *Molecular Phylogenetics and Evolution*, **69**, 63–74.

Pabijan M, Zieliński P, Dudek K *et al.* (2015) The dissection of a Pleistocene refugium: phylogeography of the smooth newt, *Lissotriton vulgaris*, in the Balkans. *Journal of Biogeography*, **42**, 671–683.

Pinho C, Hey J (2010) Divergence with gene flow: models and data. *Annual Review of Ecology, Evolution and Systematics*, **41**, 215–230.

Poelstra JW, Vijay N, Bossu CM *et al.* (2014) The genomic landscape underlying phenotypic integrity in the face of gene flow in crows. *Science*, **344**, 1410–1414.

Pritchard JK, Stephens M, Donnelly P (2000) Inference of population structure using multilocus genotype data. *Genetics*, **155**, 945–959.

R_Development_Core_Team (2011) *R: A Language and Environment for Statistical Computing*. R Foundation for Statistical Computing, Vienna, Austria.

Rafinski J, Arntzen JW (1987) Biochemical systematics of the Old-World newts, genus *Triturus* – allozyme data. *Herpetologica*, **43**, 446–457.

Rafiński J, Cogălniceanu D, Babik W (2001) Genetic differentiation of the two subspecies of the smooth newt inhabiting Romania, *Triturus vulgaris vulgaris* and *T. v. ampelensis* (Urodela, Salamandridae) as revealed by enzyme electrophoresis. *Folia Biologica*, **49**, 239–245.

Roček Z (1994) Review of fossil Caudata of Europe. Abhandlungen und Berichte des Museums für Naturkunde und Vorgeschichte. *Magdeburg*, **17**, 51–56.

Rousset F (2008) GENEPOP'007: a complete re-implementation of the GENEPOP software for Windows and Linux. *Molecular Ecology Resources*, **8**, 103–106.

Roux C, Tsagkogeorga G, Bierne N, Galtier N (2013) Crossing the species barrier: genomic hotspots of introgression between two highly divergent *Ciona intestinalis* species. *Molecular Biology and Evolution*, **30**, 1574–1587.

Sambatti JBM, Strasburg JL, Ortiz-Barrientos D, Baack EJ, Rieseberg LH (2012) Reconciling extremely strong barriers with high levels of gene exchange in annual sunflowers. *Evolution*, **66**, 1459–1473.

Seehausen O, Butlin RK, Keller I *et al.* (2014) Genomics and the origin of species. *Nature Reviews Genetics*, **15**, 176–192.

Sjödin P, Kaj I, Krone S, Lascoux M, Nordborg M (2005) On the meaning and existence of an effective population size. *Genetics*, **169**, 1061–1070.

Slatkin M (2005) Seeing ghosts: the effect of unsampled populations on migration rates estimated for sampled populations. *Molecular Ecology*, **14**, 67–73.

Sousa V, Hey J (2013) Understanding the origin of species with genome-scale data: modelling gene flow. *Nature Reviews Genetics*, **14**, 404–414.

Sousa VC, Beaumont MA, Fernandes P, Coelho MM, Chikhi L (2012) Population divergence with or without admixture: selecting models using an ABC approach. *Heredity*, **108**, 521–530.

Storey JD (2002) A direct approach to false discovery rates. *Journal of the Royal Statistical Society Series B: Statistical Methodology*, **64**, 479–498.

Storey JD, Tibshirani R (2003) Statistical significance for genomewide studies. *Proceedings of the National Academy of Sciences of the United States of America*, **100**, 9440–9445.

Strasburg JL, Rieseberg LH (2010) How robust are "isolation with migration" analyses to violations of the im model? A simulation study. *Molecular Biology and Evolution*, **27**, 297–310.

Stuglik MT, Babik W (in press) Genomic heterogeneity of historical gene flow between two species of newts inferred from transcriptome data. *Ecology and Evolution*, doi:10.1002/ece3.2152

Sweigart AL, Mason AR, Willis JH (2007) Natural variation for a hybrid incompatibility between two species of *Mimulus*. *Evolution*, **61**, 141–151.

Tajima F (1989) Statistical method for testing the neutral mutation hypothesis by DNA polymorphism. *Genetics*, **123**, 585–595.

Teeter KC, Thibodeau LM, Gompert Z *et al*. (2010) The variable genomic architecture of isolation between hybridizing species of house mice. *Evolution*, **64**, 472–485.
Wakeley J (2004) Metapopulation models for historical inference. *Molecular Ecology*, **13**, 865–875.
Wakeley J (2009) *Coalescent Theory. An Introduction*. Roberts, Greenwood Village.
Wakeley J, Aliacar N (2001) Gene genealogies in a metapopulation. *Genetics*, **159**, 893–905.
Wegmann D, Leuenberger C, Excoffier L (2009) Efficient approximate Bayesian computation coupled with Markov chain Monte Carlo without likelihood. *Genetics*, **182**, 1207–1218.
Wegmann D, Leuenberger C, Neuenschwander S, Excoffier L (2010) ABCtoolbox: a versatile toolkit for approximate Bayesian computations. *BMC Bioinformatics*, **11**, 116.
Weir BS, Cockerham CC (1984) Estimating F-statistics for the analysis of population structure. *Evolution*, **38**, 1358–1370.
Weisrock DW, Macey JR, Ugurtas IH, Larson A, Papenfuss TJ (2001) Molecular phylogenetics and historical biogeography among salamandrids of the "true" salamander clade: rapid branching of numerous highly divergent lineages in *Mertensiella luschani* associated with the rise of Anatolia. *Molecular Phylogenetics and Evolution*, **18**, 434–448.
Wielstra B, Arntzen JW (2011) Unraveling the rapid radiation of crested newts (*Triturus cristatus* superspecies) using complete mitogenomic sequences. *BMC Evolutionary Biology*, **11**, 162.
Wright S (1931) Evolution in Mendelian populations. *Genetics*, **16**, 97–159.
Yatabe Y, Kane NC, Scotti-Saintagne C, Rieseberg LH (2007) Rampant gene exchange across a strong reproductive barrier between the annual sunflowers, *Helianthus annuus* and *H. petiolaris*. *Genetics*, **175**, 1883–1893.
Zieliński P, Nadachowska-Brzyska K, Wielstra B *et al.* (2013) No evidence for nuclear introgression despite complete mtDNA replacement in the Carpathian newt (*Lissotriton montandoni*). *Molecular Ecology*, **22**, 1884–1903.
Zieliński P, Dudek K, Tadeusz Stuglik M, Liana M, Babik W (2014a) Single nucleotide polymorphisms reveal genetic structuring of the Carpathian newt and provide evidence of interspecific gene flow in the nuclear genome. *PLoS One*, **9**, e97431.
Zieliński P, Stuglik MT, Dudek K, Konczal M, Babik W (2014b) Development, validation and high-throughput analysis of sequence markers in nonmodel species. *Molecular Ecology Resources*, **14**, 352–360.

W.B. and P.Z. designed the research. P.Z. and K.D. performed the laboratory procedures. P.Z. and K.N-B. contributed analytical tools. P.Z. and W.B. analysed the data. P.Z. and W.B. wrote the manuscript (with contribution from other authors).

Data accessibility

Variant calling (VCF) files and alignments of sequenced markers are available on Dryad Digital Repository: doi:10.5061/dryad.83k00.

Supporting information

Additional supporting information may be found in the online version of this article.

Table S1 Sampling sites. Number of individuals sampled for polymorphism data (N) and demographic analysis (ABC) are given.

Table S2 Prior and posterior distribution of M3 model.

Table S3 Prior and posterior distribution of VS.RGF model for LvIN – LvOUT comparison.

Table S4 Within-species nucleotide diversity (π) and Tajima's D calculated for each gene separately.

Table S5 Nucleotide diversity calculated within (diagonal) and between populations.

Table S6 Population differentiation.

Table S7 Observed summary statistics for three groups (Lm-LvIN-LvOUT).

Table S8 Observed summary statistics for two groups comparisons.

Table S9 Performance of three-group models applying constant population sizes and constant gene flow.

Table S10 Overall power of three-population model selection procedure for models applying constant population sizes and constant gene flow.

Table S11 Power of three-population model selection procedure for models assuming constant population sizes and constant gene flow estimated in the observed summary statistics space.

Table S12 Overall power of two-population model selection procedure.

Table S13 Power of two-population model selection procedure estimated in the observed summary statistics space.

Table S14 Performance of three-group models allowing for a single demographic change in each population and recent gene flow.

Table S15 Overall power of three-group model selection procedure for models allowing for a single demographic change in each population and recent gene flow.

Table S16 Power of three-group model selection procedure for models allowing for a single demographic change in each population and recent gene flow estimated in the observed summary statistics space.

Fig. S1 Localities sampled for demographic analyses (details in Table S1).

Fig. S2 The three-group models investigated in the study.

Fig. S3 Nucleotide diversity and divergence measures within and between populations of *Lissotriton montandoni* (1–31) and *L. vulgaris* (32–69) Nucleotide diversity shown on the diagonal as the average number of nucleotide positions differing between a pair of homologous sequences within a population.

Fig. S4 Genetic differentiation between populations of *L. montandoni* (1–31) and *L. vulgaris* (32–69).

Fig. S5 Identification of the number of groups (K) in Structure analysis for *L. montandoni* and *L. vulgaris*.

Fig. S6 Parameters estimated from best three-population model - M3 (migration between Lv groups and between LvIN and Lm).

Fig. S7 Posterior probabilities of the parameters inferred from best three-population model M3.

Fig. S8 Distributions of posterior quantiles of all the parameters inferred from best three-population model M3.

Fig. S9 Parameters estimated from best LvIN – LvOUT two-group model – VS.RGF (demographic change and recent migration).

Fig. S10 Posterior probabilities of the parameters inferred from best Lm – Lv two-group model – VS.RGF.

Fig. S11 Posterior probabilities of the parameters inferred from best Lm – LvOUT two-group model – VS.RGF.

Fig. S12 Posterior probabilities of the parameters inferred from best Lm – LvIN two-group model – VS.RGF.

Fig. S13 Posterior probabilities of the parameters inferred from best LvIN – LvOUT two-group model – VS.RGF.

Fig. S14 Distributions of posterior quantiles of all the parameters inferred from best Lm – Lv two-group model – VS.RGF.

Fig. S15 Distributions of posterior quantiles of all the parameters inferred from best Lm – LvIN two-group model – VS.RGF.

Fig. S16 Distributions of posterior quantiles of all the parameters inferred from best Lm – LvOUT two-group model – VS.RGF.

Fig. S17 Distributions of posterior quantiles of all the parameters inferred from best LvIN – LvOUT two-group model – VS.RGF.